Supporting Mechanism and Effect of Artificial Pillars in a Deep Metal Mine

Z. Kang, Z. Hongyu, Z. Junping, W. Xiaojun, Z. Kui

Abstract. The supporting mechanism for overburden strata supported by artificial pillars is a complex issue. A calculation method for the size optimization of an artificial pillar in a deep area based on Protodyakonov's ground pressure theory was proposed. In this study, the sizes of artificial pillars in different mining sections in a specific mine were calculated. In addition, the stability of these artificial pillars and the supporting effect for the overburden strata in the gob areas were studied. First, the size parameters of the artificial pillars in different mining sections were determined. Second, the supporting mechanism and stability of the artificial pillars were studied by means of numerical calculation. A regular pattern in which a larger gob area span corresponds to greater settlement of the overburden strata were found. The overburden strata are stable based on the distribution condition of the plastic zone. Finally, field measurements were performed, revealing continuous increases in both the pressure borne by the artificial pillars in two middle sections at the primary stage and the settlement displacement of the overburden strata. After reaching a certain level, the increasing trend slowed and finally plateaued. The maximum stress of the artificial pillar at a depth of -430 m was 0.78 MPa, and its maximum relative settlement of the overburden strata was 4.4 mm. Similarly, the maximum stress of the artificial pillar at a depth of -460 m was 0.43 MPa, and its maximum relative settlement of the overburden strata was 2.7 mm. The study results showed that the designed artificial pillars are capable of supporting the overburden strata with good stability in the mining process and can effectively prevent the destruction of surrounding rocks and overburden strata in the gob area for the purpose of supporting the mine.

Keywords: great depth, overburden strata, artificial pillar, supporting mechanism, mechanical characteristics.

1. Introduction

With the gradual reduction of mineral resources, adopting artificial pillars instead of natural pillars to support overburden rocks has become increasingly important. The overburden strata around the goaf are supported by artificial pillars instead of ore pillars in rare and precious metal mines. However, these pillars have different supporting mechanisms, resulting in an unclear movement mechanism for overburden strata supported by artificial pillars and threatening the mine safety. Few studies have been conducted on the instability mechanism of overburden strata around the goaf (Liu *et al.*, 2013; Chen & Zhou, 2010). Because the supporting abilities of artificial pillars are influenced by complex factors, including filling technologies, filling material properties and design strength, their supporting performance often falls short of expectations (Gu & Li, 2006; Luo *et al.*, 2010; Ghasemi *et al.*, 2012). Many scholars have studied the design of artificial pillars; among their findings are indications that changing the ratio and adding new materials can improve the strength of the filling pillar (Tu *et al.*, 2014; Lind, 2005; Palei & Das, 2009). However, studies on improving the strength of artificial pillars have progressed slowly due to the restrictions of the field conditions and filling processes as well as high filling costs. Based on the relevant literature domestically and abroad, the strength of artificial filling pillars is generally less than 5 MPa. Conventionally, the size of an artificial pillar is determined according to area bearing capacity theory (Brady & Brown, 2006), which calls for larger artificial pillars for deeper mining depths. However, this theory does not fully take into account relevant factors that may affect the reasonable size of the artificial pillar, resulting in excessively wide backstoping pillars in deep areas, a waste of filling materials and increased filling cost. Therefore, in this study, the supporting mechanism is investigated, and a new design method is developed to determine the size of the artificial pillar.

2. Mechanical Model of the Artificial Pillar

When the room and pillar method is used in the mining process, the length of the artificial pillar is generally the

Zhao Kang, PhD., Associate Professor and Deputy Director of Civil and Mechanics Laboratory Center, School of Architectural and Surveying Engineering, Jiangxi University of Science and Technology, Ganzhou 341000, China. e-mail: zhaok_666666@163.com.
Zhao Hongyu, MSc., Student, School of Architectural and Surveying Engineering, Jiangxi University of Science and Technology, Ganzhou 341000, China. e-mail: zhaohongyu@163.com.
Zhang Junping, MSc., Student, School of Architectural and Surveying Engineering, Jiangxi University of Science and Technology, Ganzhou 341000, China. e-mail: 1192991685@qq.com.
Wang Xiaojun, PhD., Associate Professor and Director of Mining Engineering Department, School of Architectural and Surveying Engineering, Jiangxi University of Science and Technology, Ganzhou 341000, China. e-mail: wangxiaojun@163.com.
Zhao Kui, PhD., Full Professor and President, School of Architectural and Surveying Engineering, Jiangxi University of Science and Technology, Ganzhou 341000, China. e-mail: Yglmf-zk@163.com.
Submitted on March 15, 2015; Final Acceptance on August 7, 2015; Discussion open until December 31, 2015.

inclined length in the middle section, and the height is the thickness of the ore body. Both are determined by the occurrence conditions of the ore body. Therefore, the width of the artificial pillar is the design key for the structural parameters in this mining method. Based on the bearing theory of artificial pillars (Fig. 1), the weight of the overburden rock within the plastic zone without a pressure arch must first be determined. Each middle section is divided into rooms and pillars in the orebody trend in the mining process. The backstoping is completed in two steps: Step 1 is backstoping the pillar and then refilling concrete into the pillar as a whole, and Step 2 is backstoping the room between the concrete pillars. According to the Protodyakonov's ground pressure theory, the radius of the plastic zone can be expressed as (Wang *et al.*, 2012; Cai, 2002; Diederichs *et al.*, 2002)

$$R_p = R_0\left[\frac{(P_0 + c\cos\varphi)(1-\sin\varphi)}{c\cot\varphi}\right]^{\frac{1-\sin\varphi}{2\sin\varphi}} \quad (1)$$

In this formula, R_0 is the excavation radius, m; P_0 is the vertical gravity stress of the mining depth, MPa; c is the cohesive force of the rock, MPa; and φ is the internal friction angle of the rock, °.

Experimental results show that the plastic zone radius (R_p) is affected slightly by the excavated sectional form. In calculations, R_p can be approximated by the equivalent excavated radius, *i.e.*, the circumradius of the different sectional forms. As for the ore block, the equivalent excavated radius (R_0) can be obtained as follows.

R_0 and P_0 are calculated with the following formulas:

$$R_0 = \sqrt{\left(\frac{L}{2}\right)^2 + \left(\frac{h}{2}\right)^2} \quad (2)$$

$$P_0 = \gamma H \quad (3)$$

The load intensity of the top pressure within the unit length without the pressure arch is:

$$q_d = \gamma\left(R_p - \frac{h}{2}\right) \quad (4)$$

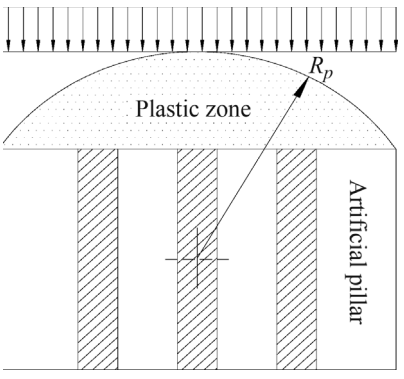

Figure 1 - Schematic diagram of the pillar bearing mechanism.

In this formula, q_d is the load intensity of the top pressure within the unit length without the pressure arch, kN/m; γ is the unit weight of the surrounding rock, kN/m^3; and h is the height of the mining space, m.

In the calculation of the total load, the mining span must be maximal. Therefore, the whole mining span must be considered to obtain the total load within the mining span above the artificial pillar.

$$Q_d = q_d \times L \quad (5)$$

In this formula, Q_d is the total load, kN; L is the span of the mining space, m, namely, the total length along the strike of the ore body; H is the depth of the mining space, m.

Equations 2 and 3 are substituted into Eq. 1 to give R_p.

According to strength theory, the width of the artificial pillar is determined by its own strength, the pressure borne by the artificial pillar and the dead-weight. Due to the impact of the filling process and the site conditions, the strength values of the artificial pillar can be obtained by reducing the pilot testing values.

$$\sigma \le \frac{S_p}{n} = [\sigma] \quad (6)$$

In this formula, S_p is the intensity value of the sample of the artificial pillar tested in the laboratory, MPa; σ is the average stress of the artificial pillar, MPa; $[\sigma]$ is the permissible stress of the artificial pillar, MPa; and n is the strength reduction factor, which is determined by the actual site conditions and construction technology. n varies between 1.5 and 2.

The unit length of the artificial pillar is used to calculate:

$$\frac{Q_d + NQ_m}{NB} \le \sigma \quad (7)$$

In this formula, N is the number of the artificial pillars; B is the width of the artificial pillar, m; Q_m is the dead-weight of the unit length of every artificial pillar, kN.

$$Q_m = Bh\gamma_1 \quad (8)$$

where γ_1 is the init weight of the artificial pillar.

The calculation formula of the width of the artificial pillar can be determined by solving Eqs. 1-8 simultaneously:

$$B = \frac{n\gamma L\left[(L^2 + h^2)^{\frac{1}{2}}\left[\left(\frac{(\gamma H + c\cot\varphi)(1-\sin\varphi)}{c\cot\varphi}\right)\right]^{\frac{1-\sin\varphi}{2\sin\varphi}} - h\right]}{2N(S_p - nh\gamma_1)} \quad (9)$$

Considering the effects of the ratio of the geometric shapes, such as the effect of the aspect ratio on the bearing capacity of the artificial pillar, the width of the artificial pillar must be corrected (Ji, 1991):

$$B_C = B\sqrt{\frac{h}{B}} = \sqrt{BH} \quad (10)$$

Based on Eqs. 9 and 10, the calculation formula for the width of the artificial pillar can be obtained. In the design of the width of the artificial pillar, the width must be provisionally estimated based on different numbers of artificial pillars. The calculation result is then compared with the actual locations of the mine rooms and artificial pillars to determine the most reasonable width for the artificial pillar.

3. Example of the Jiaochong Mine, China

The gold mine in Jiaochong, China, is 500 m beneath the ground with a surface elevation of +160 m. The length of the ore body is 90 m with an average thickness of 5 m. It is mined by the room and pillar method, and artificial pillars are used to replace natural pillars to ensure the stability of the surrounding rocks of the gob area. The mine is divided into seven mining sections: -390 m, -410 m, -430 m, -460 m, -500 m, -540 m and -580 m. Currently, the sections above -410 m are finished. Backstoping has been performed in the section at -430 m. The section at -460 m is developed. Due to the impact of the surface environment, the main well is arranged in the region of the theoretical moving zone. Therefore, studying the effect of the mining processes of the sections at -430 m and -460 m on the overburden surrounding rocks and the surface movement is important, making the study of the size design and the stability of the artificial pillar crucial. The strike length of the mine section at -430 m is -85 m. The strike length of the mine section at -460 m is -65 m. The average inclination angle of the ore body is 30°. To ensure the stability of the surrounding rocks in the gob area and the reasonable design of the structural parameters of the ore blocks, a reasonable size for the artificial pillar must be determined. The physical and mechanical parameters of the overburden rock and mine backfill and the mining depth and spans are substituted into Eq. 9, developed by the author, and the corrected Eq. 10 with different selected N values for the trial calculation gives the following results:

Reasonable size of the artificial pillar in the section at -430 m:

$$B_{-430} = 6.6015 \text{ m} \quad N=4$$

Reasonable size of the artificial pillar in the section at -460 m:

$$B_{-460} = 5.7713 \text{ m} \quad N=3$$

4. Analysis of the Supporting Mechanism and Stability Effect of the Artificial Pillar

4.1 Supporting mechanism and mechanical characteristics

To verify the stability of the designed artificial pillar and the supporting effect for the overburden rocks in the gob area, the stability of the artificial pillar and the moving conditions of the overburden rocks in the sections at -430 m and -460 m were studied. The dimensional parameters of the mine rooms and the artificial pillars (with concrete used as the filling material) can be seen in Table 1, and the layout can be seen in Fig. 2.

Numerical modeling of the case study was performed using the finite difference modeling software FLAC^{3D} by Itasca. The mine has a bottom buried depth of 790 m, 124614 nodes and 117096 units. The physical and mechanical parameters of the model are shown in Table 2. The dimensions of the model are 600 m 600 m 400 m (Fig. 3). A gradient mode is adopted for meshing, with more dense and even grids used in the areas emphasized in this research. The model uses displacement boundary conditions: using the roll around support ($u_x = 0$, $u_y = 0$) and fixing the bottom ($u_x = 0$, $u_y = 0$, $u_z = 0$), the upper boundary is the gravity stress of the overburden rock (σ_{zz} = -10.92 MPa), the horizontal stress in the direction of the ore body tendency is 1.25 times the vertical stress ($\sigma_x = 12.5\ \sigma_z$), and the horizontal stress along the ore body is 0.75 times the vertical stress along the run of ore body ($\sigma_x = 0.75\ \sigma_z$). The Mohr-Coulomb strain softening standards are used in the calculations.

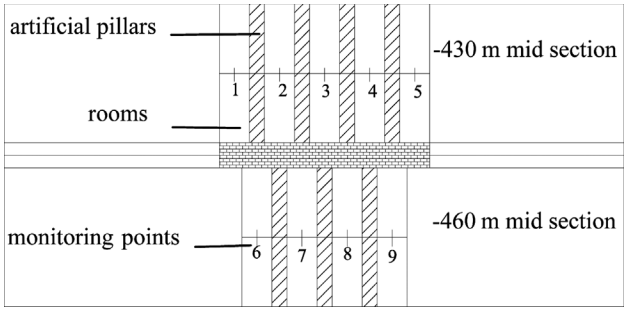

Figure 2 - Schematic diagram of the stope structure positions and the monitoring points in different sections.

Table 1 - Parameter design for the ore block structure.

Mid-section	Ore block structure parameter			
	Number of pillars per section	Pillar width (m)	Number of rooms per section	Room width (m)
-430 m	4	6.6	5	11.7
-460 m	3	5.8	4	11.9

Table 2 - Mechanical parameters of the rock mass.

Constituent	Unit weight (kN/m^3)	Elastic modulus (MPa)	Cohesion (MPa)	Friction angle (°)	Poisson's ratio	Tensile strength (MPa)
Surrounding rock	28	60000	15	45	0.2	7.5
Ore body	27.1	65000	15	42	0.19	7.5
Artificial pillar	21	230	0.171	35	0.25	0.01

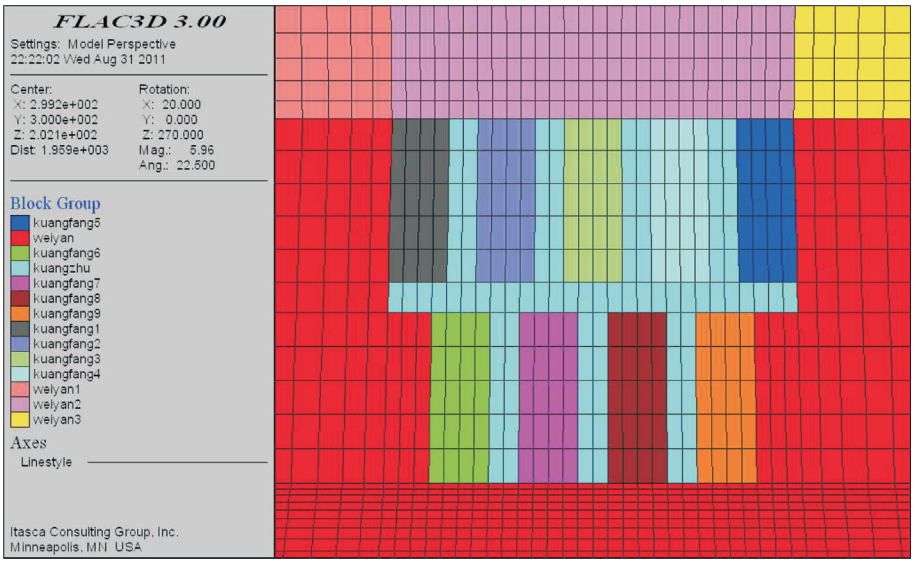

Figure 3 - Model of the mine rooms and artificial pillars.

In the mining process, the stress was significantly changed, especially in the area of the surrounding rocks outside the mine rooms at both ends. The stress in the bottom of the area of the surrounding rocks outside the mine rooms reached 61.03 MPa (Fig. 4), which was less than the maximum compressive strength of the surrounding rock, 75 MPa. However, in these areas, the safety monitoring should be enhanced and reinforcement measures should be implemented to ensure safety. According to the diagram of the maximum principal stress, the strain of the artificial pillar is relatively stable, without stress concentration (Zhao, 2012). The pressure on the pillar is also less than its compressive strength. The damage of any material starts with the appearance of a plastic zone. After the completion of mining, the artificial pillar had no plastic zones. Only two of the sections had plastic zones in the mining process. After the two sections were finished, the stress on the artificial pillar was stable, which indicates that the structural parameters of the designed artificial pillar can better prevent the formation and destruction of plastic zones in the overburden rocks in the gob area. The stress diagram and the plastic zone distribution show that the compressive stress or tensile stress is less than the breaking strength of instability, which will prevent the instability of the overburden rocks and the failure of the artificial pillar itself. The plastic zone distribution diagram of the mine rooms and overburden rocks also shows the superior supporting effect of the artificial pillar and the relatively stable stoping structures.

The stability and supporting effect of the artificial pillar are reflected by the displacement of the mine roof panels. To study the stability and supporting effect of the artificial pillar, displacement monitoring points #1-#5 were set up in the middle of the roof panel inside the mine room in the section at -430 m, and displacement monitoring points #6-#9 were set up in the middle of the roof panel inside the mine room in the section at -460 m. According to the calculation results, after the mining in the two sections was completed, monitoring point #3 in the roof panel inside the mine room in the section at -430 m had a maximum displacement settlement of 8.02 mm. Points #6 and #9 in the roof panels inside the two mine rooms on both ends of the gob area had a relatively small displacement settlement of 4.86 mm. Although the settlement of the roof panels in the gob area was relatively large, the stability of the roof panels was minimally affected based on the plastic zone distribution of the roof panels. After the section at -460 m was mined completely, monitoring points #7 and #8 of the roof panel in the gob area had a maximum settlement of 7.76 mm and a minimum settlement of 5.30 mm. Comparing the maximum values of the settlement in these two

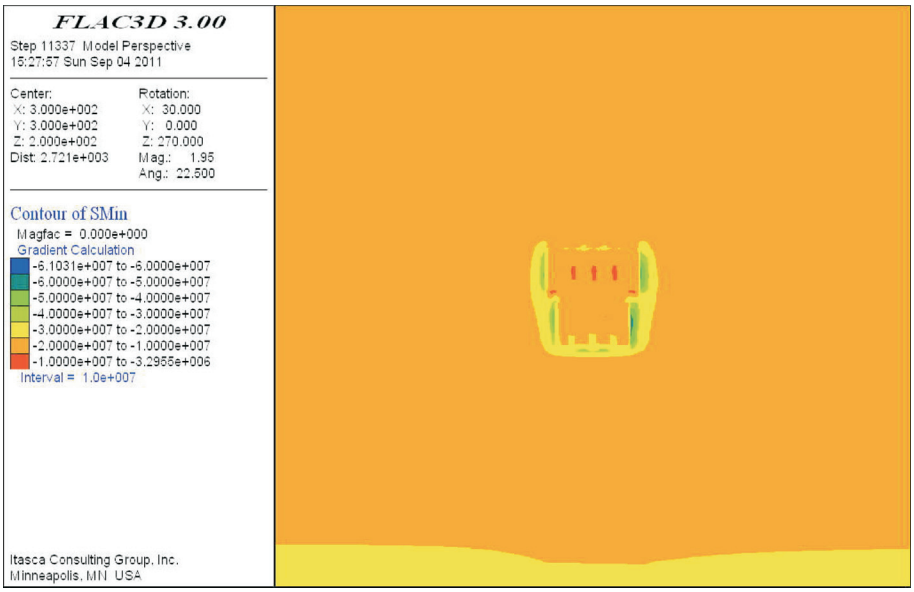

Figure 4 - Contour map of maximum principal stress.

sections, it can be observed that the settlement of a roof panel in a mine room is closely related to the section span such that larger spans correspond to greater settlement (the span of the section at -430 m is 85 m, and the span of the section at -460 m is 65 m).

4.2 Discussion of the field measurement supporting effect

The parameters in Table 1 show that although the backstoping depth of the section at -460 m is larger than that of the section at -430 m, its backstoping span is smaller. Therefore, the width is much more influential than the backstoping depth. According to Eqs. 9 and 10 established by the author, the reasonable width of the artificial pillar in the section at -460 m is less than that in the section at -430 m. To verify the practicality and rationality of the design, the monitoring data from the actual site are used to determine whether the design can meet the safety requirements. Therefore, monitoring equipment was set up in the mining sections. To study the supporting effect of the designed artificial pillar, the stress of the overburden rock, the displacement and the acoustic emission were monitored.

The stress variation status of the artificial pillar was monitored by vibrating wire strain gauges. After finishing the backstoping of the first-stage artificial pillar in the sections at -430 m and -460 m, a concrete pressure gauge was set up in the bottom of the striped uphill before filling the artificial pillar. The monitoring values of the concrete pressure gauge were recorded during and after the second-stage backstoping process. The stress variations and stress variation rates were obtained from the monitoring results to determine the areas with potential stress concentration and destruction. The monitoring results provide a reference basis to analyze the destruction type or the destruction scope of the artificial pillar or overburden rock. A sudden rise of the stress variation rate or a stress approaching the ultimate strength of the overburden rock can be regarded as an instability criterion for the artificial pillar or overburden rock.

Stress monitoring was conducted for nine months with concrete pressure gauges in these two sections (monitoring in the section at -430 m started in January 2008, and monitoring in the section at -460 m started in January 2009). The stress monitoring graph (Fig. 5) shows that the pressure of the roof panels on the top of the artificial pillar increased during the backstoping of the mine rooms at both ends. After completing the backstoping, the pressure variation curve plateaus. This result indicates the variation distribution of the vertical pressure of the artificial pillar used to bear the weight of overburden rocks. Based on the monitoring values, the maximum vertical stress of the artificial pillar in the section at -430 m is 0.78 MPa, and the maximum vertical stress of the artificial pillar in the section at -460 m is 0.43 MPa. Compared to the designed width of the artificial pillar according to the above formula, the width of the artificial pillar in the section at -430 m is larger than that in the section at -460 m, which is due to the larger mining span of the section at -430 m. Therefore, the on-site monitoring data indicate that the mining span of the artificial pillar is more influential than the mining depth.

The displacement in the sections at -430 m and -460 m was monitored with a VWM-type vibrating wire multipoint displacement meter. The displacement monitoring was performed for eight months for the roof panels in the gob area of the mine rooms (monitoring in the section at -430 m started in August 2009, and monitoring in the section at -460 m started in April 2010). Monitoring holes were drilled in the roof panels inside the gob area of the mine rooms. The relative amount of subsidence, collapse

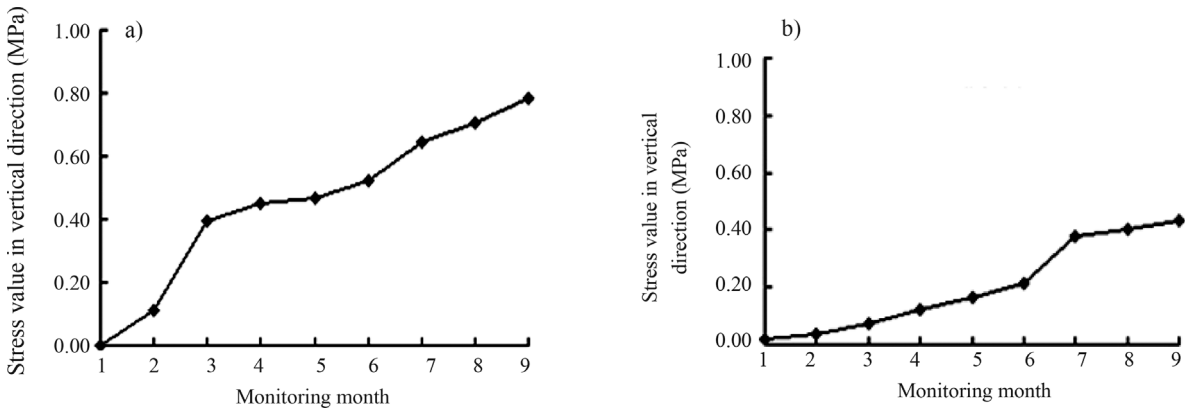

Figure 5 - Monitoring results recorded by the pressure gauge. (a) Stress monitoring of the artificial pillar in the section at -430 m. (b) Stress monitoring of the artificial pillar in the section at -460 m.

degree and destruction extent can be obtained through monitoring. When the monitoring holes are relatively deep, the bottom of the hole with a small displacement amount is regarded as the monitoring reference point. A sudden rise of the variation rate in multiple monitoring points or a sudden rise of the displacement value can be considered as the instability criterion of the overburden rock.

Typical monitoring data for the roof panels in the mine room of the two sections were selected for analysis. In the early months of the backstoping, the settlement amount of the roof fluctuated, and the settlement amount was also large. When the stress of the overburden rock in the mine rooms was transferred to the artificial pillar, the settlement amount of the roof decreased and gradually leveled off (Fig. 6). This result indicates that the movement patterns of the overburden rock controlled by artificial pillars with different widths are the same. They all exhibit a large amount of settlement in the primary stage. The settlement data feature more sudden fluctuations. When the distribution of the stress of the overburden rock becomes more stable, the settlement change of the roof in the gob area is also stable and can meet the safety requirements. Different distances from the hole bottom result in different relative displacements, with greater distances from the hole bottom (that is, shorter distances from the orifice) leading to greater relative displacement. The difference in the roof settlement in these two sections is reflected in the following aspects. First, larger gob area backstoping spans correspond to larger amounts of roof settlement. For example, the maximum relative settlement in the section at -430 m is 4.4 mm, and the maximum relative settlement in the section at -460 m is 2.7 mm. The settlement monitoring curve indicates that a larger span causes larger jumps in the settlement amount (the maximum absolute difference between the two groups of the monitoring data in the section at -430 m is approximately 0.8 mm, and the maximum absolute difference between the two groups of the monitoring data in the section at -460 m is approximately 0.5 mm), which indicates that the variation is large, with strong instability. Second, a larger backstoping span of the gob area results in a longer fluctuation cycle time of the displacement settlement curve. The main cause of this phenomenon is the large span, which results in a long stress redistribution duration for the roof and transfers to different directions during the stress redis-

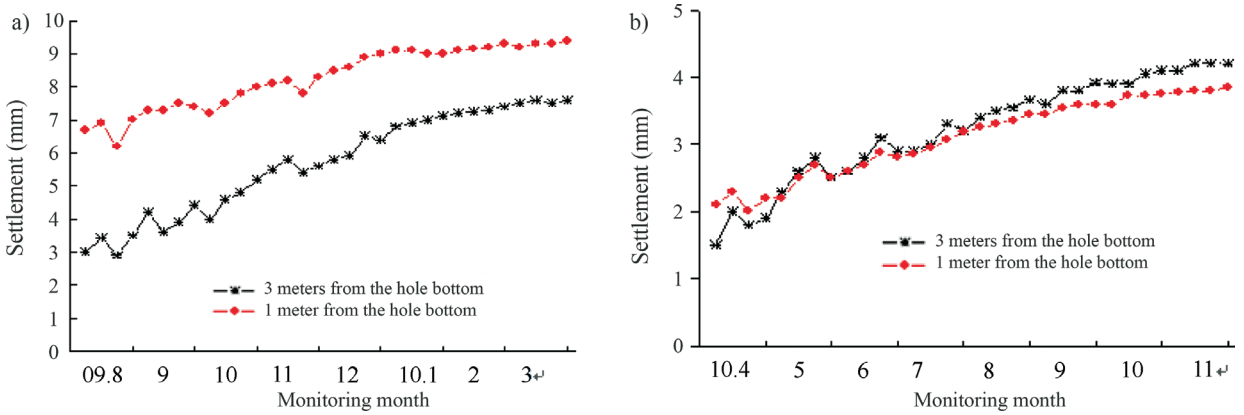

Figure 6 - Monitoring results obtained from the multipoint displacement meter. (a) Displacement monitoring of the mine room roof in the section at -430 m. (b) Displacement monitoring of the mine room roof in the section at -460 m.

tribution. In addition, the stress becomes more concentrated on the artificial pillars on both sides as time passes. A smaller span will lead to shorter stress redistribution time and more regular transfers of the stress distribution. The stress is more easily transferred to the focal points of stress, namely, both sides of the artificial pillar.

Such parameters as acoustic emission frequency and energy of rock mass can reflect the destruction process of the mass to some extent. In geotechnical engineering, the acoustic emission monitoring technique mainly evaluates and predicts the stability of rock mass using three indexes: total events, large events and energy rate. Because the span in the section at -430 m is relatively large and has many instability factors, the acoustic emission monitors were only set up in the key surrounding rocks of the gob area in this section. The monitoring data acquired by the acoustic emission probe at a certain period of time were selected for analysis. Table 3 shows that only a few sporadic acoustic emission signals of the overburden rock are observed in the absence of outside interference. The acoustic emission energy is small, and the acoustic emission phenomenon is infrequent and of short duration, which indicates that the monitored overburden rock in the gob area is stable.

Table 3 - A portion of the acoustic emissions monitoring data.

Monitoring time	Number of large events/Φ	Number of total events/N	Energy rate /E	Notes	Monitoring time	Number of large events/Φ	Number of toatal events/N	Energy rate /E	Notes
2010.01.12/00:10:44	0	0	0		2010.01.12/10:00:00	20	46	157	Period of preparation for rock drilling
2010.01.12/00:11:05	0	0	0		2010.01.12/10:00:21	4	12	35	
2010.01.12/00:11:27	0	0	0		2010.01.12/10:00:43	1	10	41	
2010.01.12/00:11:49	0	0	0		2010.01.12/10:01:04	1	3	16	
2010.01.12/00:11:59	0	0	0		2010.01.12/10:01:15	0	0	0	
2010.01.12/00:12:10	0	0	0		2010.01.12/10:01:25	0	0	0	
2010.01.12/00:12:20	0	0	0		2010.01.12/10:35:41	67	186	692	
2010.01.12/00:12:42	0	0	0		2010.01.12/10:36:03	45	78	725	
2010.01.12/00:12:53	0	0	0		2010.01.12/10:41:00	25	67	176	
2010.01.12/00:13:03	**1**	**3**	**6**		2010.01.12/10:41:10	47	120	0	
2010.01.12/00:20:00	0	0	0		2010.01.12/10:41:20	1	23	675	
2010.01.12/00:20:23	0	0	0		2010.01.12/10:41:42	89	143	832	
2010.01.12/00:20:33	0	0	0		2010.01.12/10:41:52	50	100	256	
2010.01.12/00:20:44	**1**	**1**	**1**		2010.01.12/10:42:03	47	66	0	
2010.01.12/00:20:55	0	0	0		2010.01.12/10:42:14	87	143	164	
2010.01.12/00:21:06	0	0	0		2010.01.12/10:42:25	99	146	240	
2010.01.12/00:21:27	0	0	0		2010.01.12/10:42:46	37	66	386	
2010-01-12/00:21:38	0	0	0		2010-01-12/10:42:56	14	24	365	
2010-01-12/00:21:48	0	0	0		2010-01-12/10:44:10	21	67	503	
2010-01-12/00:22:09	**3**	**5**	**7**		2010-01-12/10:44:32	55	167	647	
2010-01-12/00:22:21	0	0	0		2010-01-12/10:44:42	78	143	868	
2010-01-12/00:22:31	0	0	0		2010-01-12/10:44:53	99	169	1044	
2010-01-12/00:22:53	0	0	0		2010-01-12/10:57:00	43	156	678	
2010-01-12/00:23:03	0	0	0		2010-01-12/10:57:10	67	157	967	
2010-01-12/00:30:12	0	0	0		2010-01-12/10:57:32	43	67	654	
2010-01-12/00:30:33	0	0	0		2010-01-12/10:57:53	23	43	303	
2010-01-12/00:30:44	0	0	0		2010-01-12/10:58:04	34	54	878	

Period without mining disturbance

Period of rock drilling blasting and ore-drawing

5. Conclusion

(1) A new calculation method is proposed for the design of rational artificial pillar dimensions for deep mining. This method can compensate for the shortcomings of setting the dimension parameters of artificial pillars according to area bearing capacity theory. It can also provide a reference basis for the design of artificial pillars, optimize the pillar dimensions, and reduce the artificial pillar filling cost in mines.

(2) According to the numerical results, the compressive stress or tensile stress experienced by the artificial pillar is much lower than the compressive strength or tensile strength, which indicates that the artificial pillar is stable. With the support of the artificial pillar, the settlement of the overburden rock roof in the gob area is controlled. The maximum displacement settlement amount is 8.02 mm in the roof panel inside the mine room in the section at -430 m, and the maximum displacement settlement amount is 7.76 mm in the roof panel inside the mine room in the section at -460 m, which does not affect the stability of the artificial pillar and the roof overburden rock.

(3) The on-site monitoring data reveal that the vertical stress of the artificial pillar in the section at -430 m is larger than that in the section of -460 m, which indicates that the impact of the mining span of the artificial pillar exceeds the mining depth.

(4) When the backstoping span in the gob area is large, there is a larger settlement of the overburden rock roof, the settlement fluctuation is greater, and the overburden rock is more unstable. Additionally, the larger the backstoping span, the longer the period of the re-distribution process of the roof and the settlement cycle.

(5) In the absence of outside interference, only a few sporadic acoustic emission signals of the overburden rock appear. The acoustic emission is characterized by low energies and a short duration, which indicates that the monitored overburden rock in the gob area is stable.

(6) The various study methods used show that the structural parameters of the designed artificial pillar are reasonable and can effectively prevent movement of the overburden rock in the gob area to meet safety requirements.

Acknowledgments

The authors gratefully acknowledge the National Natural Science Foundation of China (Grant 51304083), the Science and Technology Program of Jiangxi Province (20132BBG70106), the Jiangxi Province Science Foundation for Youths (20142BAB216020), and the Natural Science Foundation of Jiangxi University of Science and Technology (NSFJ2014-K02).

References

Brady, B.H. G. & Brown, E. T. (2006). Rock Mechanics for Underground Mining. Third edition. Kluwer Academic Publishers, New York, 377 p.

Cai, M.F. (2002). Rock Mechanics and Angineering. Science Press, Beijing: 126 p (in Chinese).

Chen, Q.F. & Zhou, K.P. (2010). Action mechanism of low-grade backfill on stability of mining environment structure. Rock and Soil Mechanics, 31(9):2811-2816.

Diederichs, M.S.; Coulson, A.; Falmagne, V.F.; Rizkala, M. & Simser, B. (2002). Application of rock damage limits to pillar analysis at Brunswick Mine. In: Proceedings of the North American Rock Mechanics Conference, UTPress, Toronto, pp. 1325-1332.

Ghasemi, E.; Ataei, M.; Shahriar, K.; Sereshki, F.; Jalali, S.E. & Ramazanzadeh, A. (2012). Assessment of roof fall risk during retreat mining in room and pillar coal mines. International Journal of Rock Mechanics and Mining Sciences, 54:80-89.

Gu, D.S. & Li, X.B. (2006). Modern Mining Science and Technology for Metal Mineral Resources. Metallurgical Industry Press, Beijing, 235 p.

Ji, W.D. (1991). Mining Rock Mechanics. Metallurgical Industry Press, Beijing, 38 p.

Liu, C.L.; Tan, Z.X.; Deng, K.Z. & Li, P.X. (2013). Synergistic instability of coal pillar and system and filling method based on plate model. International Journal of Mining Science and Technology, 23:145-149.

Lind, G. (2005). An integrated risk management approach for underground coal pillar extraction in South Africa. Journal of the South African Institute of Mining and Metallurgy, 105(2):137-147.

Luo, H.; Yang, S.J. & Tao, G.Q. (2010). Stability analysis of ore pillar and application using concept of dynamic fuzzy reliability based on Finite Element Method Artificial Neural Network-Monte Carlo Simulation. Journal of China Coal Society, 35(4):551-554.

Palei, S.K. & Das, S.K. (2009). Logistic regression model for prediction of roof fall risks in bord and pillar workings in coal mines: An approach. Safety Science, 47(1):88-96.

Tu, H.S.; Tu, S.H.; Zhang, X.G.; Li, Z.X. & Jia, S. (2014). Technology of back stoping from level floors in gateway and pillar mining areas of extra-thick seams. International Journal of Mining Science and Technology, 24:143-149.

Wang, X.J.; Feng, X.; Zhao, K.; Yang, T.B. & Zhao, K. (2012). Reasonable width calculation and analysis of artificial pillar in deep mining. Journal of Mining & Safety Engineering, 29(1):54-59.

Zhao, K. (2012). Study of Overburden Movement Mechanism and Prevention in Jiaochong Gold Mine. Ph.D. Thesis, University of Science and Technology, Beijing,79 p (in Chinese).